Chapter 3: EXPERIMENTAL PROCEDURE

This chapter explains the experimental procedures and the techniques used to synthesize and characterize the reinforcements like reduced graphene oxide (rGO), Ni-doped reduced graphene oxide (rGO-Ni), Ni-doped hexagonal boron nitride (*h*-BN-Ni), and Ni alloy-based self-lubricating composites reinforced with solid lubricants. It also includes the details of the procedure and parameters adopted to evaluate the friction and wear behaviour of composites as well as base alloy. The techniques like FESEM, EDS, XRD, and Raman spectroscopy implemented to characterize the worn surfaces of the tribo-pair after friction and wear testing.

3.1 RAW MATERIALS

Table 3.1 gives the size, purity and supplier information for the various powders and chemicals used in the current study.

Table 3. 1 Powders, their size, purity, and supplier

Material	Size	Purity	Supplier
Nickel (Ni) powder	325 mesh	99.8%	Otto chemi, Maharashtra, India.
Chromium (Cr) powder	<40 μm	99.9%	
Molybdenum (Mo) powder	30-40 μm	99.0%	Nanoshel, Wilington, UK
Titanium (Ti) powder	40-50 μm	99.0%	
Silver (Ag) powder	40-50 μm	99.0%	
Hexagonal boron nitride (*h*-BN) powder	60 nm	99.5%	
Aluminium (Al) powder	7-15 μm	99.5%	Alfa Aesar, Wardhill, MA, USA
Sodium nitrate ($NaNO_3$)	-	98.0%	
Graphite powder	< 20 μm	-	Sigma Aldrich, St. Louis, MO, USA
Nickel chloride hexahydrate ($NiCl_3.6H_2O$)	-	99.9%	

Hydrazine hydrate		50-60%	
Potassium permanganate ($KMnO_4$)	-	99.0%	Merck, Darmstadt, Germany
Hydrogen chloride (HCl)	-	37.0%	
Sulfuric acid (H_2SO_4)	-	98.0%	
Sodium hydroborate ($NaBH_4$)	-	95.0%	
Hydrogen peroxide (H_2O_2)	-	30.0%	Loba Chemie, Maharastra, India
Liquid ammonia (NH_3)	-	25.0%	Qualikems, Gujrat, India

3.2 SYNTHESIS OF REINFORCEMENTS

3.2.1 Reduced Graphene Oxide (rGO) and Ni-doped rGO (rGO-Ni)

The schematic diagram for the synthesis of GO and rGO with the addition of rGO-Ni has been shown in Fig. 3.1. The GO was synthesized by harsh oxidation of graphite powder, in which graphite powder (10 g) and $NaNO_3$ (10 g) were slowly added to H_2SO_4 (500 mL) in their subsequent order under uninterrupted stirring while maintaining the temperature of reaction vessel (round bottom flask) < 4 ºC with the aid of ice bath. It was followed by gradually adding 60 g $KMnO_4$ in the reaction vessel placed on the ice bath under continuous stirring. After 24 hours, the reaction vessel was transferred to an oil bath, and 700 mL of distilled water was added very slowly to this highly oxidized acidic reaction mixture (Caution: highly exothermic reaction). Subsequently, the temperature of the reaction vessel was increased to 98 ºC under uninterrupted stirring for rigorous oxidation of graphite powder into graphite oxide. After 24 hours, the temperature of the oxidizing reaction mixture was brought down to room temperature, and 120 ml of H_2O_2 was gradually added to quench the oxidation reactions, followed by washing of the product with 90 mL HCl for the saturation and solubilization of unused potassium permanganate. The brown oxidized product, i.e., graphite oxide, was thoroughly washed with several cycles of

distilled water until the pH of the decanted water became neutral. The graphite oxide dispersed in water was exfoliated into GO with the aid of an ultrasonic probe. The exfoliated aqueous dispersion was centrifuged at 5000 rpm for 20 minutes to separate the supernatant having highly dispersible GO sheets from the partially exfoliated product (precipitate in centrifuge tubes). The GO dispersion was used for further processing and analyses.

The rGO was prepared by chemical reduction of highly dispersed GO in an aqueous medium. In this context, 200 ml GO dispersion (GO concentration: 2.5 mg/mL) was charged in the reaction vessel kept in an oil bath. A solution of 5 mL hydrazine hydrate was added to the GO dispersion under continuous stirring, and the temperature of the reaction mixture was raised to 98 ºC for the reduction of GO sheets. After 24 hours of reduction, the temperature of the reaction vessel was brought back to room temperature, and the developed black product, i.e., rGO was thoroughly separated via membrane filtration and washed with distilled water for several cycles. The wet cake of rGO was dried at 80 ºC.

The Ni-based nanoparticles were grown on a graphene skeleton via a wet chemistry route to improve its interfacial interaction with the metal matrix. In this process, 100 mL aqueous solution of 2 g $NiCl_3.6H_2O$ was rigorously mixed with 150 ml aqueous dispersion of GO (3.3 mg/mL) under uninterrupted stirring in the round bottom flask, placed in oil bath, which forms an aqueous complex of nickel, i.e., $[Ni\ (H_2O)_6]^{2+}$ over the thoroughly dispersed GO nanosheets. It was followed by the addition of liquid ammonia (20 mL) and hydrazine hydrate (20 mL) in the reaction mixture under continuous stirring to form a $[Ni\ (NH_3)_6]^{2+}$ complex. After 2 hours, 0.2 g $NaBH_4$ was added to the reaction mixture, and the chemical reduction reaction was allowed to occur for 12 hours. The synthesized black

dispersion of reduced graphene oxide decorated with Ni-nanoparticles (rGO-Ni) was separated with the aid of an external magnetic field and repeatedly washed with distilled water until the pH of the washed-out water became neutral. The wet cake of rGO-Ni was dried at 80 °C to get rGO-Ni in powder form to be used as reinforcement for preparing the composites.

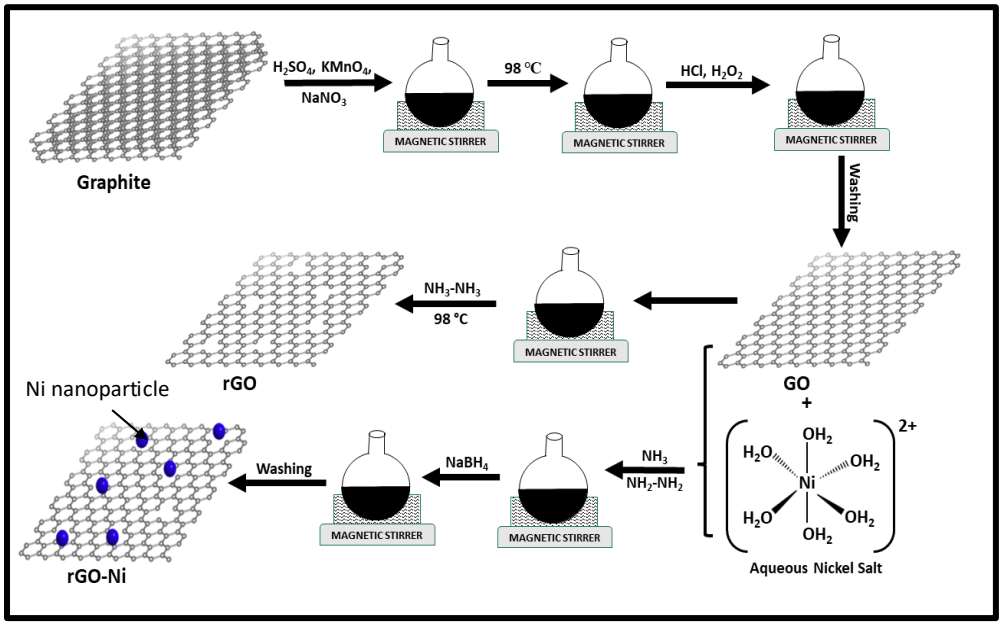

Fig. 3. 1 Synthesis of GO, rGO, and Ni-doped rGO via wet chemistry routes

3.2.2 Ni-doped Hexagonal Boron Nitride (*h*-BN-O-Ni)

In the first step, the *h*-BN nano powder was oxidized to generate oxygen functionalities and structural defects on the surface of the *h*-BN lamellae. The *h*-BN is a chemically stable material. Therefore, it was oxidized with highly aggressive oxidants to generate oxygen functionalities. In this context, *h*-BN nano powder (7 g) and $NaNO_3$ (7 g) were gradually added to H_2SO_4 (350 mL) under uninterrupted stirring. The temperature of the reaction vessel was maintained at ≤ 4 °C with the aid of an ice bath. It was followed by a gradual addition of 42 g $KMnO_4$ in the reaction vessel (*Caution: Highly exothermic reaction*) under continuous stirring in an ice bath. After 24 hours of oxidation process at

ambient temperature, the reaction vessel was placed in an oil bath, and 500 mL distilled water was gradually added to the oxidative reaction mixture (*Caution: Highly exothermic reaction*) under interrupted stirring. Subsequently, the temperature of the reaction vessel was raised to 98 ºC for thorough oxidation of *h*-BN nano powder. After 24 hours, the temperature of the oxidizing reaction mixture was brought to ambient condition, and then 84 mL H_2O_2 was progressively added to freeze the oxidation reactions. The oxidized product was washed with 49 mL HCl to mineralize the leftover $KMnO_4$ in the reaction mixture. The oxidized *h*-BN (*h*-BN-O) was washed thoroughly with numerous cycles of distilled water until the pH of the decanted water became neutral, and then the wet cake of *h*-BN-O was dried at 70 ºC. The steps followed are depicted in Fig. 3.2.

The nickel nanoparticles were grown on the surface of *h*-BN-O lamellae via the wet chemistry route. In this process, 100 mL aqueous solution of $NiCl_3.6H_2O$ (2.0 g) was thoroughly mixed with 150 mL aqueous dispersion of *h*-BN-O (0.5 g) under uninterrupted stirring in the round bottom flask. The $NiCl_3.6H_2O$ formed a nickel-hydrated complex on the surface of hydroxyl functionalities-enriched *h*-BN-O. Subsequently, liquid ammonia (20 mL) and hydrazine hydrate (20 mL) were added, and the reaction mixture was stirred for 2 hours to form a $[Ni\ (NH_3)_6]^{2+}$ complex. It was followed by the addition of $NaBH_4$ (0.2 g) for further chemical reduction of $[Ni\ (NH_3)_6]^{2+}$ complex on the surface of *h*-BN-O. During the reduction process, green dispersion gradually converted into a black product, i.e., *h*-BN-O decorated with Ni nanoparticles (*h*-BN-O-Ni). The *h*-BN-O-Ni was separated using an external magnetic field and repeatedly washed with distilled water until the pH of the washed-out water became neutral. The wet cake of *h*-BN-O-Ni was dried at 70 ºC for further analyses and the preparation of composites.

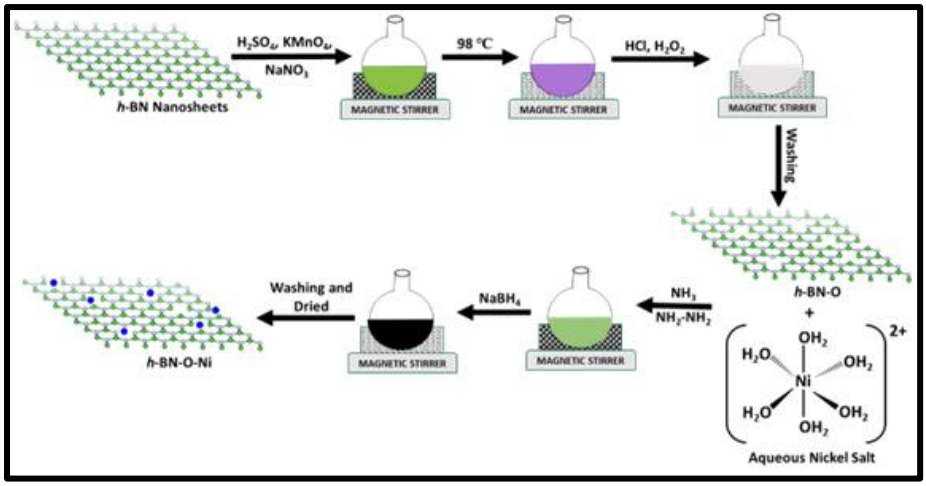

Fig. 3. 2 A schematic demonstration of stepwise preparation of *h*-BN-O and *h*-BN-O-Ni

3.2.3 Characterisation of rGO, rGO-Ni, and *h*-BN-Ni

3.2.3.1 *Fourier-transform infrared spectrometer (FTIR) analysis*

The various linkages and chemical functional groups in the GO, rGO, rGO-Ni, *h*-BN, *h*-BN-O, and *h*-BN-O-Ni were probed by collecting their vibration spectra using a Fourier-transform infrared (FTIR) spectrometer (Spectrum-Two, PerkinElmer Inc., Shelton, USA). The KBr pellet of each sample was prepared to collect the FTIR spectrum at a resolution of 4 cm^{-1}.

3.2.3.2 X-ray diffraction (XRD) analysis

The crystallinity and phase purity of rGO, rGO-Ni, and *h*-BN-O-Ni were subjected to X-ray diffraction (Model: Rigaku Miniflex 600 Desktop X-Ray Diffraction System; Make: RIGAKU Corporation, Tokyo, Japan) with Cu Kα monochromatic source at a voltage of 40 kV and current of 15 mA. XRD patterns were taken in a 2θ range of 10–110° with 0.02° step size and 2°/min scan speed. The data analyses were performed by using Xpert Highscore software.

3.2.3.3 Raman spectroscopy

The structural features of the synthesized rGO and rGO-Ni were analysed using Raman spectroscope (Model: LabRAM HR Evolution Raman spectrometer; Make: Horiba Scientific, SAS-Lille, Japan France) equipped with a diode laser (λ = 532 nm excitation) over a range of 100-4000 cm^{-1} at a 100 X magnification of objective lens with a grating of 600 groves per mm.

3.2.3.4 Transmission electron microscopy (TEM)

The microscopic features, including the lamellar pattern of rGO, *h*-BN, and distribution (size and shape) of Ni nanoparticles in rGO-Ni and *h*-BN-O-Ni were analysed by their micrographs captured using a transmission electron microscope (Model: JEM-2100; Make: JEOL, Tokyo, Japan).

3.2.3.5 X-ray photoelectron spectroscopy (XPS)

The surface composition and chemical environment of rGO, rGO-Ni, *h*-BN-O, and *h*-BN-O-Ni were examined using high-resolution X-ray photoelectron spectra (XPS) of each constituent element, along with survey spectra, were examined by X-ray photoelectron spectroscope (Model: K Alfa; Make: Thermo Fisher Scientific, Waltham, MA, USA) equipped with Mg Kα line as an X-ray source. The spectra were acquired in the binding energy of 185-195, 275-300, 385-410, 520-544, and 840-890 eV for B 1s, C 1s, N 1s, O 1s, and Ni 2p, respectively with 20 number of scans, whereas the survey spectra were recorded in the binding energy of 1350-0 eV with 3 scans. The high-resolution spectra of each element for these samples were fitted by applying the Shirley background.

3.3 FABRICATION OF Ni ALLOY AND COMPOSITES

The individual powders of Ni, Cr, Mo, Ti, and Al were mixed in specific weight percentages for mechanical alloying process of base alloy (N0). The composition of these powders was as follows: 67 wt.% Ni, 15 wt.% Cr, 10 wt.% Mo, 5 wt.% Ti, and 3 wt.% Al. The powder mixture was milled for 10 hrs using ball mill (VBCC Ceramics, Chennai, India) with zirconia balls (Jayashree Spheres & Measures, Pune, India), having diameter of 8 mm and hardness of 70 HRC, along with 1% ethanol maintaining a ball-to-powder ratio of 10:1. The milled powder mixtures were dried in vacuum and put in a properly cleaned graphite die (Nickunj Eximp Enterprises Pvt. Ltd, Mumbai, Maharashtra, India) having an internal diameter of 30 mm. Graphite foil of 0.5 mm thickness was used on the top, bottom, and cylindrical surface of the punch to facilitate easy removal of the specimen from the graphite die. Subsequently, the composites were sintered using a spark plasma sintering furnace (Dr. Sinter SPS-625, Fuji Electronic, Japan). The mixed powder was heated at a rate of 100 ºC/min under a sintering pressure of 55 MPa in an argon atmosphere followed by furnace cooling. During the sintering process, the temperature was maintained steady for 5 minutes at two different instances: first at 600 ºC and second at the sintering temperature (i.e., 1000 ºC). The sintered specimens were carefully removed from the die punch assembly using a hydraulic press. The composites were fabricated under similar conditions. The designation and sintering parameters of the composites used are given in Table 3.2.

Table 3. 2 Designation, composition and spark plasma sintering parameters of Ni alloy-based composites

Sample Designation	Ni alloy (wt.%)	Ag (wt.%)	rGO (wt.%)	rGO-Ni (wt.%)	*h*-BN-Ni (wt.%)	SPS parameters		
						Sintering Pressure (MPa)	Maximum Temperature (°C)	Heating Rate (°C/min)
N0	100	0	0.0	0.0	0	55	1000	100
NA	90	10	0.0	0.0	0			
NAG	89	10	1.0	0.0	0			
NANG/ NANG1.0	89	10	0.0	1.0	0			
NANG0.5	89	10	0.0	0.5	0			
NANG1.5	88	10	0.0	1.5	0			
NANG2.0	88	10	0.0	2.0	0			
NAh2	88	10	0.0	0.0	2			
NAh4	86	10	0.0	0.0	4			
NAh6	84	10	0.0	0.0	6			
NAh8	82	10	0.0	0.0	8			
NANGh2	87	10	0.0	0.0	2			
NANGh4	85	10	0.0	0.0	4			
NANGh6	83	10	0.0	0.0	6			
NANGh8	81	10	0.0	0.0	8			

3.3.1 Characterization of Base Alloy and Composites

The crystallinity and phase purity of sintered base alloy/ composites were examined using XRD analysis. The morphology of the elemental powders, ball-milled powders, sintered base alloy and the worn surfaces of the tribo-pairs after sliding were examined under a field emission scanning electron microscope (Model: Nova Nano SEM 450, Make:

FEI Company of USA) equipped with Energy-dispersive spectroscopy (EDS).

3.3.2 Hardness and Density Measurement

The microhardness of the base alloy and all the composites have been measured by a pyramid-shaped diamond indenter having an included angle of 136º at an indentation load of 300 g and dwell time of 10 seconds using a semi-automatic microhardness tester (Micro Mach Technologies, Pune, (Maharashtra), India) following ASTM E384 standards. At least ten indentations have been made at different locations, and the average value has been reported as the hardness of the composite. The density of the sintered base alloy and composites were measured thrice using the Archimedes method in accordance with ASTM: B9621-3 standards, under an open atmosphere in the water medium, and its average value has been reported.

3.4 DRY FRICTION AND WEAR TEST

The friction and wear tests on the base alloy and composite, namely, NA, NAG, NANG/NANG1.0, NANG0.5, NANG1.5, NANG2.0, NAh2, NAh4, NAh6, NAh8, NANGh2, NANGh4, NANGh6, and NANGh8, were conducted using a High temperature Uni-directional Rotary Tribometer (Model: TR-20LE-DHM-PHM-800; Make: DUCOM, Bangalore, India) against a stationary silicon-nitride ball (Si_3N_4, having diameter of 6 mm) following ASTM G99-95 standards. Each test was conducted at RT, 200, 400, 600, and 800 °C at a constant load of 5 N and fixed sliding speed of 0.5 m/s. Each composite specimen was polished with emery sheets up to a grit size of 1200, followed by cloth polishing with alumina before being subjected to a wear test. The surface roughness value of the specimens before the wear test was estimated to be 0.05 μm. All the tests were conducted at 35 to 55 % relative humidity. All the tests were run for 40 minutes, corresponding to a sliding

distance of 1200 m. Each test was done thrice, and the average data has been reported. After each run, the tribometer and induction heater were switched off and left to cool to ambient temperature before the sample was weighed. The mass loss of the specimen was measured using a microbalance (A & D instruments, India) having an accuracy of 1×10^{-7} kg. The specific wear rate of the disc was calculated using the following formula.

$$\text{Specific wear rate } (mm^3/\text{Nm}) = \frac{\text{Wear Volume } (mm^3)}{\text{Applied load (N)} \times \text{Sliding distance (m)}} \qquad (3.1)$$

The calibration of the torque on the sample was done in terms of the friction force as specified on the instrument, using a constant distance of the lever arm of the apparatus. The measurement of frictional force was done in the tribometer using a computerised data acquisition system and strain gauge force transducer. The frictional force was recorded continuously by a computer. The coefficient of friction has been evaluated from the friction force and the normal loads; only pre-calibrated dead loads have been used.

The schematic diagram of a high temperature ball-on-disc tribometer setup is shown in Fig. 3.3. The tribometer equipped with an induction heater that heated the rotary disc from the bottom. After mounting the testing specimen and the Si_3N_4 ball in their respective fixtures, the specimen was heated to the desired testing temperature with the help of an induction heater before being loaded against the Si_3N_4 counterface. The requisite load was applied to the arm after achieving the desired temperature, and the ball and composite specimen were brought into contact. The pyrometer was used to ensure that the appropriate temperature was maintained. The frictional force during each test was documented through a data acquisition system in a computer that had an interface with a tribometer. The data from the start to the end of the test has been used to estimate the coefficient of friction. The

tribometer and induction heater were switched off, left to cool to ambient temperature, and the sample was weighed after each completion of each test.

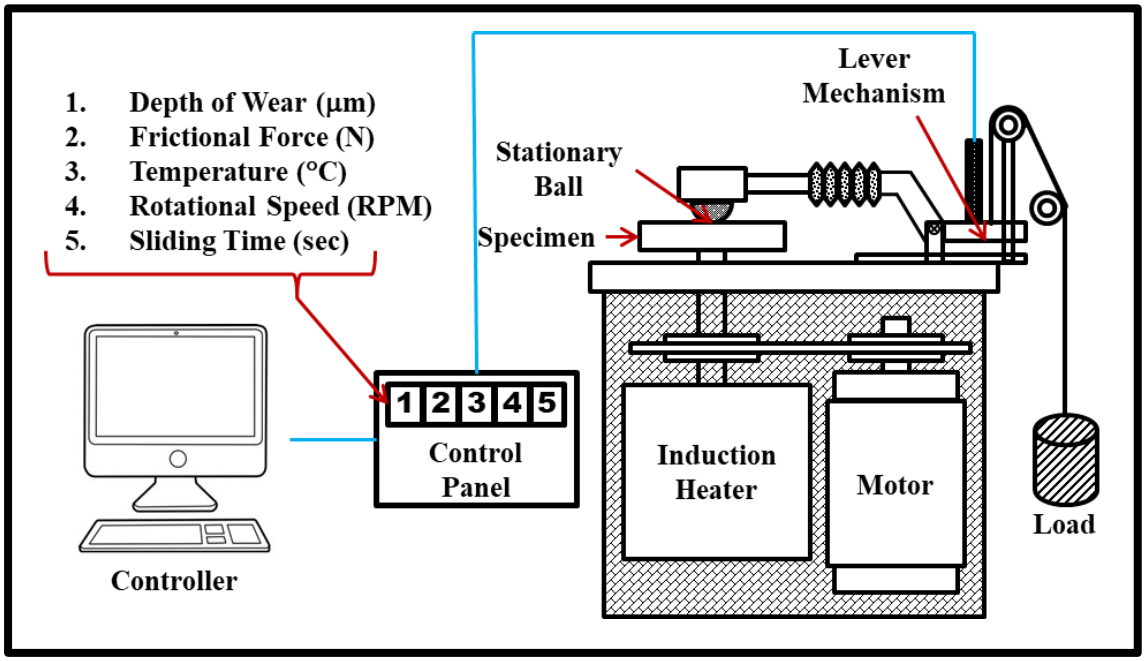

Fig. 3. 3 Schematic diagram of high temperature ball-on-disc tribometer

3.4.1 Characterization of Worn Surfaces

The presence of the phases on worn surfaces of the base alloy/composites were examined using XRD, FESEM with EDS and Raman spectroscopy. The worn surfaces of the counter balls have been examined using FESEM. Additionally, the cross-section of the subsurface of the composites were analysed using FESEM.